Hindawi
Advances in Civil Engineering
Volume 2019, Article ID 9250472, 11 pages
https://doi.org/10.1155/2019/9250472

Research Article

Experiment on Improving Bearing Capacity of Pile Foundation in Loess Area by Postgrouting

Zhijun Zhou and Yuan Xie

School of Highway, Chang'an University, Xi'an 710064, China

Correspondence should be addressed to Yuan Xie; xieyuan@chd.edu.cn

Received 10 April 2019; Accepted 21 July 2019; Published 14 August 2019

Academic Editor: Giulio Dondi

Postgrouting technology is an inevitable trend in the development of bored piles in the loess area. To study the behavior of end resistance, lateral friction, and bearing capacity of postgrouting pile and conventional pile, the mechanism of improving the bearing capacity of postgrouting at the end of pile is analyzed by the static load failure test of pile foundation, combined with the principle of grout-soil interaction and Bingham fluid model. The results show that the grout-soil interaction enhances the strength of pile end soil and promotes the exertion of end resistance; the relative displacement of pile-soil decreases, while the lateral friction increases with the change of the interface property of pile-soil; simultaneously, the climb height of grouting is approximately the theoretical analysis value. In addition, postgrouting can obviously improve the bearing characteristics of the pile so that the settlement of the pile foundation is slowed down and the bearing capacity is increased.

1. Introduction

With the development of civil engineering to large scale and mass, more and more kinds of pile foundations are applied [1–6]. But the single technology cast-in-place pile often cannot meet the needs of the above development. Due to the inherent defects of pile forming technology (pile end sediment and lateral mud skin), end resistance and lateral friction will be significantly reduced [7]. To reduce the hidden risks such as pile end sediment and lateral mud skin, the grouting technology of foundation treatment is introduced into the pile foundation, and the postgrouting technology at the pile end emerged as the times require. Postgrouting at the pile end refers to the preembedded grouting pipe of the bored pile. After the pile is formed, the solidified grout (such as pure cement slurry and cement mortar) is evenly injected into the pile end stratum or the sealed chamber through the pregrouting device at the pile end, which solidifies the sediment at the pile end and forms a hard supporting layer to reduce the settlement of pile foundation [8–10].

As an effective measure to improve the bearing capacity, postgrouting technology at the pile end has been recognized and used widely [11, 12]. Karimi et al. [13, 14] used a truncated cone container to model the pile to study the effect of grouting on pile density and soil improvement. The results showed that grouting can improve the bearing capacity of bored piles and precast concrete piles by increasing the degree of pile-soil interaction and the density of soil around the pile [15, 16]. Liu et al. [17] introduced and studied the prestressing effect in the grouting process with a typical case. The mechanism of preloading affecting bearing capacity and lateral friction was explained in detail. Based on the statistical analysis of 50 test piles, Dai et al. [18] obtained the range of the improvement coefficient of lateral friction and pile foundation resistance of different soils and put forward the key technology and parameters of postgrouting. Thiyyakkandi et al. [19] thoroughly studied the failure mechanism of the jet grouting pile under the condition of pile end and pile side grouting. Youn and Tonon [20] took the Baso River in Texas as an example to quantify the effect of postgrouting on the performance of bored piles by the finite element method. Through the field test and numerical simulation, He et al. [21] found that the lateral stiffness and bearing capacity of the pile increased by about 110% and

100%, respectively, when spraying grouting around the pile end at 7.5D (D = pile diameter).

With the continuous development of the postgrouting technology, people have accumulated a lot of experience in engineering practice [22–25], but at the same time, there is still a lack of in-depth understanding of the mechanism of postgrouting technology reinforcement, especially in the loess area, so it is of an increasing necessity to carry out the corresponding research [26–29]. In this paper, based on the static load testing, according to the measured data and combined with theoretical methods, the mechanism of improving the bearing capacity of the postgrouting pile end is analyzed, which provides a useful reference for the design and research of similar projects in the future [30, 31].

2. Site Conditions

The test site is located at the Xi'an Xianyang International Airport dedicated motorway in Shaanxi, China, as shown in Figure 1. The in situ drilling geological data show that the upper soil layer of the test area is new loess with collapsibility. The color is yellowish brown and its thickness is about 8 meters. The new loess is uniform, slightly wet, and porous, and the wormholes and snail shells can be seen. The lower part is paleosol and old loess. The thickness of paleosols ranges from 1 m to 6 m, and it is uneven. The color of paleosols is mainly brown or brown-red, and it is hard plastic, slightly wet, with fewer macropores, and a lot of calcareous nodules in the middle and lower parts. The thickness of old loess ranges from 2 m to 15 m, and it is uniform. The color is brownish-yellow; it is hard plastic, slightly wet, and compact; and the pore is not developed. The test site can be divided into six layers according to soil texture, and the geological data are shown in Table 1.

Two rotary excavation bored piles with a diameter of 1.5 m and an effective length of 22 m are arranged. The conventional pile is S1, and the postgrouting pile is S2. Specific parameters are shown in Table 2.

2.1. Grouting Technology. As a concealed project, the postgrouting is carried out to consolidate the sediment and reinforce the soil in a certain range at the pile end, after the concrete of pile has been poured and reached a certain strength (usually 7–10 days), so as to improve the bearing capacity and control the settlement of the pile foundation.

2.1.1. Grouting Equipment and Process. The grouting machine for bored piles comprises two parts: ground grouting device and underground grouting device. The ground grouting device consists of a high-pressure grouting pump, a slurry mixer, a slurry storage tank, a ground pipeline system, and the observation instruments. The underground grouting device consists of a pile, a grouting duct, and the grouting devices at the pile end, and the postgrouting device is shown in Figure 2.

In this paper, the modified grouting pipe is employed, replacing the conventional pipe by the iron pipe. The properties of iron pipe and steel reinforcement cage are the same, which can overcome the fracture problem of the PVC

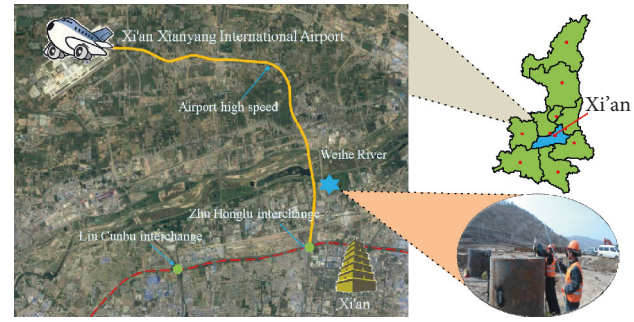

Figure 1: Test site.

pipe. The length of the thread between the two tubes is not less than 2 cm. The outer thread is wrapped with the raw rubber tape to seal the joint. The straight pipe and U-shaped pipe are evenly arranged on both sides of the reinforcing cage and tied to the inside of the reinforcing cage. Each U-shaped pipe is connected with two grouting pipes, and a check valve is arranged on the pipe. The construction process is demonstrated in Figure 3.

2.1.2. Termination Criteria of Grouting. The maximum grouting pressure is determined by the pile structure (pile length and diameter), the uplift resistance of the pile, and soil conditions. Before grouting, the maximum grouting pressure and the quality of grouting can be estimated according to the above conditions (also can be determined by experiment). Generally speaking, grouting can be terminated when the grouting quality and grouting pressure meet one of the following conditions:

(1) The grouting quality meets the design requirements

(2) The grouting quality has reached 80% of the designed value, and the grouting pressure has reached 150% of the designed grouting pressure and is maintained for more than 5 minutes

(3) The total amount of grouting has reached 80% of the design value, and there is a noticeable uplift on the top of the pile or the ground

As we all know, the soil is extremely complex. For different geological conditions, the soil properties of pile end vary greatly. This makes the grouting quality and pressure of postgrouting pile foundation differ greatly from the design requirement in the construction process. In this condition, it needs to be reanalyzed based on the actual project. It is worth noting that when the grouting pressure is very high and the grouting volume is small, it is necessary to analyze the influencing factors and eliminate the illusion caused by pipe plugging before continuing construction.

The grouting quality meets the design requirements. The quality of the final test grouting cement is 2550 kg, the maximum pressure is 2.5 MPa, and finally, the top of the pile is lifted 1.62 mm.

2.2. Measurement System. The experimental measurement system consists of displacement and stress. The former

Table 1: Geological data.

Soil	Thickness (m)	Gravity (kg/m^3)	Water content (%)	Saturation (%)	Liquid limit (%)	Liquidity index	Cohesion (kPa)	Internal friction angle (°)	Allowable bearing capacity (kPa)
Mild clay	7.5	1310	10.3	32	29.3	1.07	25.1	23	125
Silty clay	2.0	1440	12.1	50	29.5	0.87	31.5	21	125
Clay	9.4	1490	12.4	48	24.5	1.29	41.0	26	120
Mild clay	10.6	1540	13.5	52	28.8	1.27	38.9	23	132
Medium sand	12.0	1700	14.2	78	27.8	1.07	35	25	143
Medium coarse sand	14.0	2380	15.0	84	31.3	0.42	35	24	212

Table 2: Pile parameters.

Name	Number	Type	Diameter (m)	Length (m)	Remarks
S1	1	Bored pile	1.5	22	① The number of the main reinforcements is 28, and the diameter is 22 mm ② The diameter of stirrups is 8 mm, and they are arranged along the length of piles ③ The stiffening stirrups are 18 mm in diameter and 2 m in interval This is the conventional pile
S2	1	Bored pile	1.5	22	① The number of the main reinforcements is 28, and the diameter is 22 mm ② The diameter of stirrups is 8 mm, and they are arranged along the length of piles ③ The stiffening stirrups are 18 mm in diameter and 2 m in interval This is the postgrouting pile
Anchor pile	8	Bored pile	1.7	42	① The number of the main reinforcements is 32, and the diameter is 25 mm ② The diameter of stirrups is 8 mm, and they are arranged along the length of piles ③ The stiffening stirrups are 22 mm in diameter, and 2 m in interval Each anchor pile is embedded with 18 threaded steel bars with a diameter of 32 mm, which are connected with the anchor puller to provide reaction force

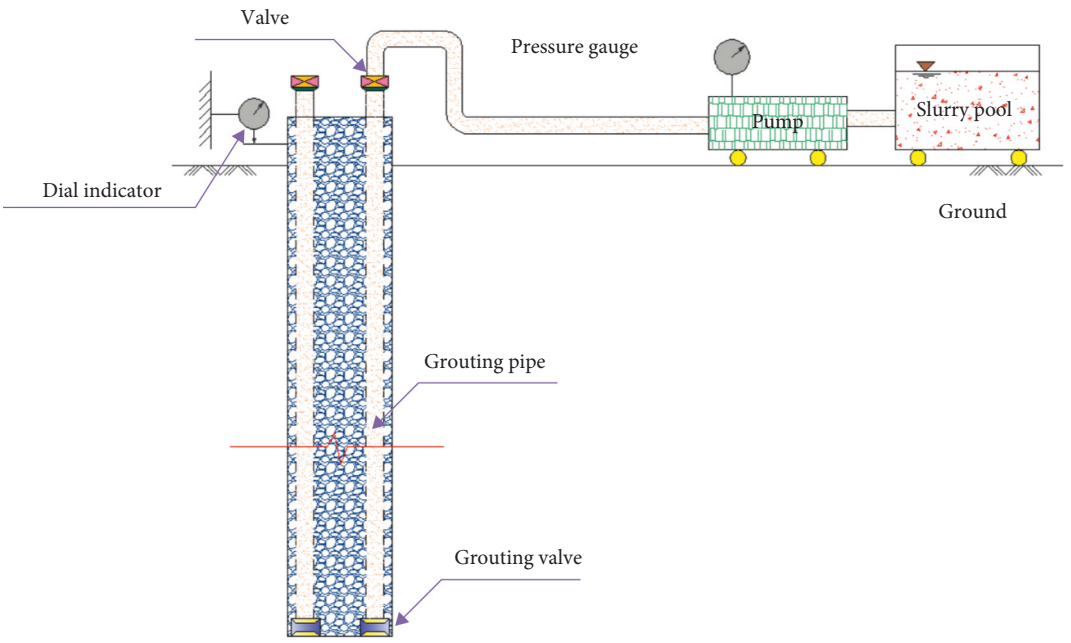

Figure 2: Schematic diagram of the grouting device.

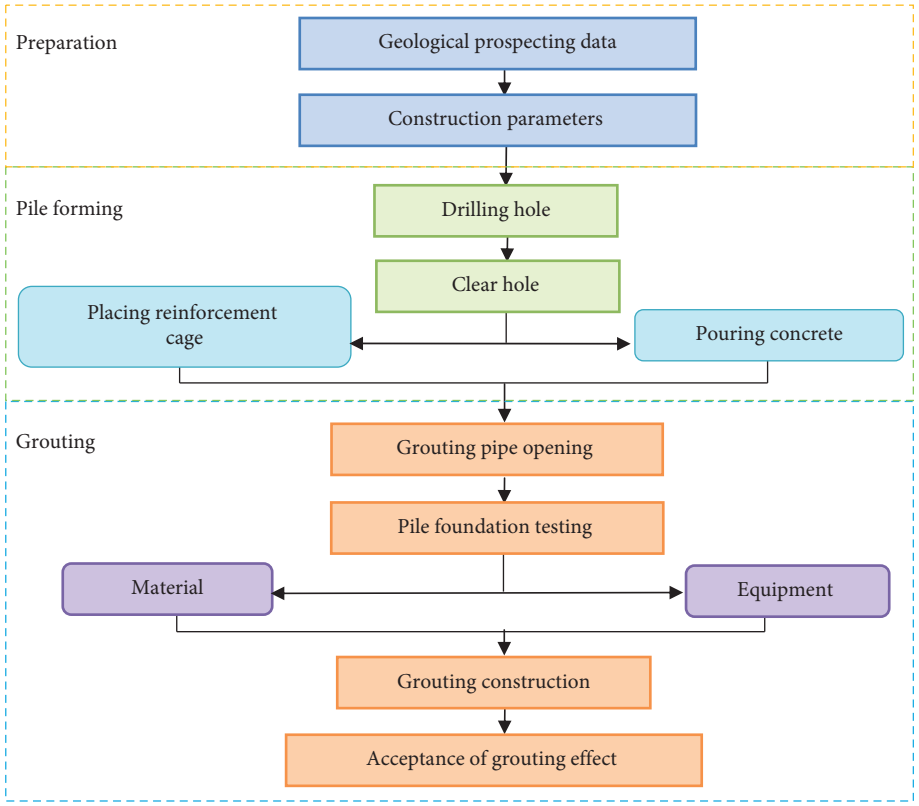

Figure 3: Grouting process.

measurement tools include the benchmark steel beam, dial indicator, and precision level. The latter includes reinforcement stress gauge and pressure box. Measuring element is an important part of the field test [32, 33]. The internal force and deformation of the pile are measured by laying instruments. The rationality of the layout of measuring instruments will affect the accuracy of the test results. In this field test, the stress and displacement of the pile are determined by using reinforcement stress gauge and dial indicator.

2.2.1. Benchmark Steel Beam and Dial Indicator. Two I-shaped benchmark steel beams are symmetrically placed on both sides of the test pile, and the nearest distance to the anchor pile is 3.3 m.

The settlement of pile foundation is measured by a dial indicator with a range of 0–100 mm. Four dial indicators are laid on the test pile plane, which are located 50 cm above the surface. They are placed in the orthogonal cross direction and fixed on the datum steel girder by a magnetic stand.

2.2.2. Reinforcement Stress Gauge and Pressure Box. JXG-1 type reinforcement stress gauge is adopted with a range of −40 kN to 60 kN and three layouts per meter. It can be put into use only after calibration. Pressure boxes are arranged on the cross section of the pile top, with five in total: one in the center of the cross section of the pile top and four in symmetrical arrangement on the vertical diameters of the piles.

2.3. Test Loading. According to the design requirements, the static load test is carried out by using counterforce device for the anchor pile crossbeam. It consists of three parts: loading system, displacement measuring system, and counterforce system. The counterforce system consists of six 500 ton hydraulic jacks: one main beam, two secondary beams, one oil pump, and four anchor piles. The loading device consists of two jacks. The loading oil pressure system is measured by the high-precision pressure gauge. The counterforce force of jacks is mainly provided by four anchor piles and main and secondary beams. It is calibrated before using the jacks.

In this static load test, the slow-speed load maintenance method is used to load step by step. After each load reaches stability, the next stage load is applied until the maximum load is reached. After being stabilized, the load will be relieved step by step until there is no load on the top of pile. Before the bearing capacity test of the single pile, each system is installed and debugged strictly according to the rules. The loading age of each test pile is 15 days.

3. Results

3.1. Bearing Capacity of Pile Foundation. As shown in Figure 4, both test piles have large vertical displacement under load and the load-displacement curve shows a "steep drop" type. The settlement of S2 is slightly greater than that of S1 at the initial stage of loading, but gradually the former is becoming smaller than the latter with the increased loading. It shows that the pile end grouting begins to play an active role. Under 17500 kN loading, the settlement of S1 is

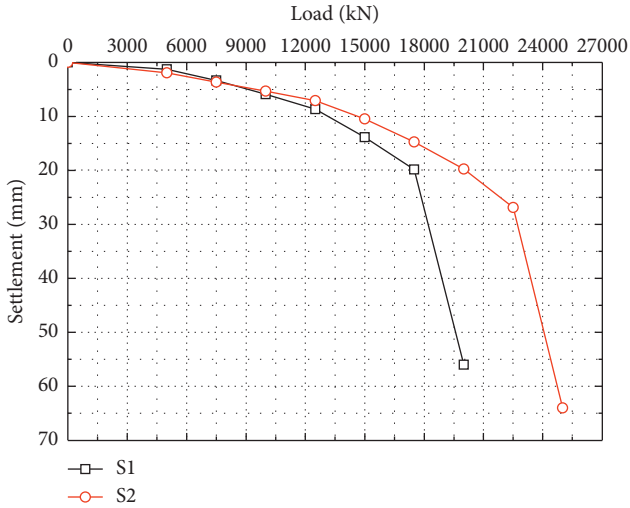

Figure 4: Load-settlement curve.

14.19 mm. Under the load of 20000 kN, the settlement of S1 suddenly increases to 57.36 mm and the pile is destroyed. At this time, the settlement of S2 is 19.77 mm and the settlement is stable, so the ultimate bearing capacity of S1 is 17500 kN. The settlement of S2 is 26.89 mm under the load of 22500 kN, and the settlement of S2 is 62.68 mm under the load of 25000 kN. The ultimate bearing capacity of S2 is 22500 kN, increased by 28.57% compared with S1. This shows that the bearing capacity of the pile foundation can be significantly improved by postgrouting at the pile end.

In the process of the postgrouting, the grout exerts an upward reaction on the test pile, resulting in upward displacement of the test pile. During the upward displacement of the test pile, the soil around the pile is disturbed and the frictional resistance of the soil layer decreases, but not significantly. Because the uplift of the test pile is 1.62 mm in the grouting process and the soil around the pile is disturbed by a single cycle under the upper load, the lateral friction of the upper soil layer plays a role first than that of the lower soil layer under the load, which makes the settlement of the postgrouting test pile slightly larger than that of the conventional pile. With the increase of load, the lateral friction of the lower soil layer is gradually exerted, and the postgrouting plays a positive role. After loading, the lateral friction of the upper soil layer decreases and the degree of decrease is greater than that of conventional piles (as shown in Figure 5), resulting in the sudden increment of settlement larger than that of the conventional pile, so the final settlement of the postgrouting pile is larger than that of the conventional pile.

3.2. Axial Force. Figures 6 and 7 are the distribution curves of axial forces of S1 and S2 test piles, respectively. It can be seen from the graph that the axial force decreases gradually downward along the pile. But in the loading stage, the decrement rate of the axial force of piles S1 and S2 is different, which is mainly manifested in the intuitive difference of the slope of the axial force curve, reflecting the size of the lateral resistance of piles. The smaller the slope is, the greater the difference of axial force is, and the greater the difference of lateral resistance between upper and lower sections at this time, which indicates that the lateral resistance of the postgrouting pile is obviously larger than that of conventional pile. And when the load is small, there is almost no axial force in the lower part of the pile. Along with the gradual increase of the load, the lower part of the pile begins to produce axial force; that is to say, the resistance at the end of the pile begins to play a role. When the pile top load reaches 22500 kN, the proportion of end resistance is about 38.02%.

3.3. Lateral Friction. As shown in Figure 5, the lateral friction begins to play a role gradually with the increased relative displacement of pile and soil [34]. Figure 5(a) shows that, due to the upward displacement of the test pile during the postgrouting process, the soil around the pile is disturbed and the lateral friction decreases to a certain extent. And under the load, the lateral friction of the upper soil layer plays a role first than that of the lower soil layer, so the decreasing degree of lateral friction of 0–4 m part of S2 is more obvious than that of S1. Because the relative displacement between pile and soil is too large, the final settlement of the test pile is larger than that of the conventional pile. The frictional resistance of 4–8 m and 8–10 m parts of the two piles increases with the increase of relative displacement of pile and soil, and the behavior of the two piles is close to each other, indicating that the effect of postgrouting on the frictional resistance of the parts is small. However, due to the overall settlement of the test pile slowed down by postgrouting, the lateral friction resistance of the parts under the ultimate load is larger than that of the conventional pile.

From Figures 5(b)–5(e), it can be seen that the lateral friction of S2 in the 10–22 m part is smaller than that of S1 at the initial loading stage when the relative displacements of pile and soil are equal, and with the increase of load, the lateral friction of S2 is larger than that of S1 when the displacements are the same. The pile and soil relative displacement of S2 is smaller than that of S1 when their lateral frictions are the same, which indicates that the postgrouting can enhance the lateral friction of this part. From 19–22 m to 10–13 m, the enhancement effect of lateral friction gradually decreases. This is due to the poor injection ability of the pile end soil in the later stage of grouting. Under the action of pressure, the grout flows upward along the pile end, and the grout pressure and flow radius decrease gradually from the pile end to upward. Therefore, the amount of grout filling between the pile side and the soil decreases upward along the pile end. The filling of cement slurry changes the interface properties of the original pile and soil so that the lateral friction of the climbing part of the slurry is enhanced, and the reinforcement effect decreases gradually from pile end to upward.

The displacement of pile end under the load decreases because of the pile end soil strengthened by postgrouting. Slurry climbing changes the interface properties of the pile and soil, the lateral friction of the climbing part increases,

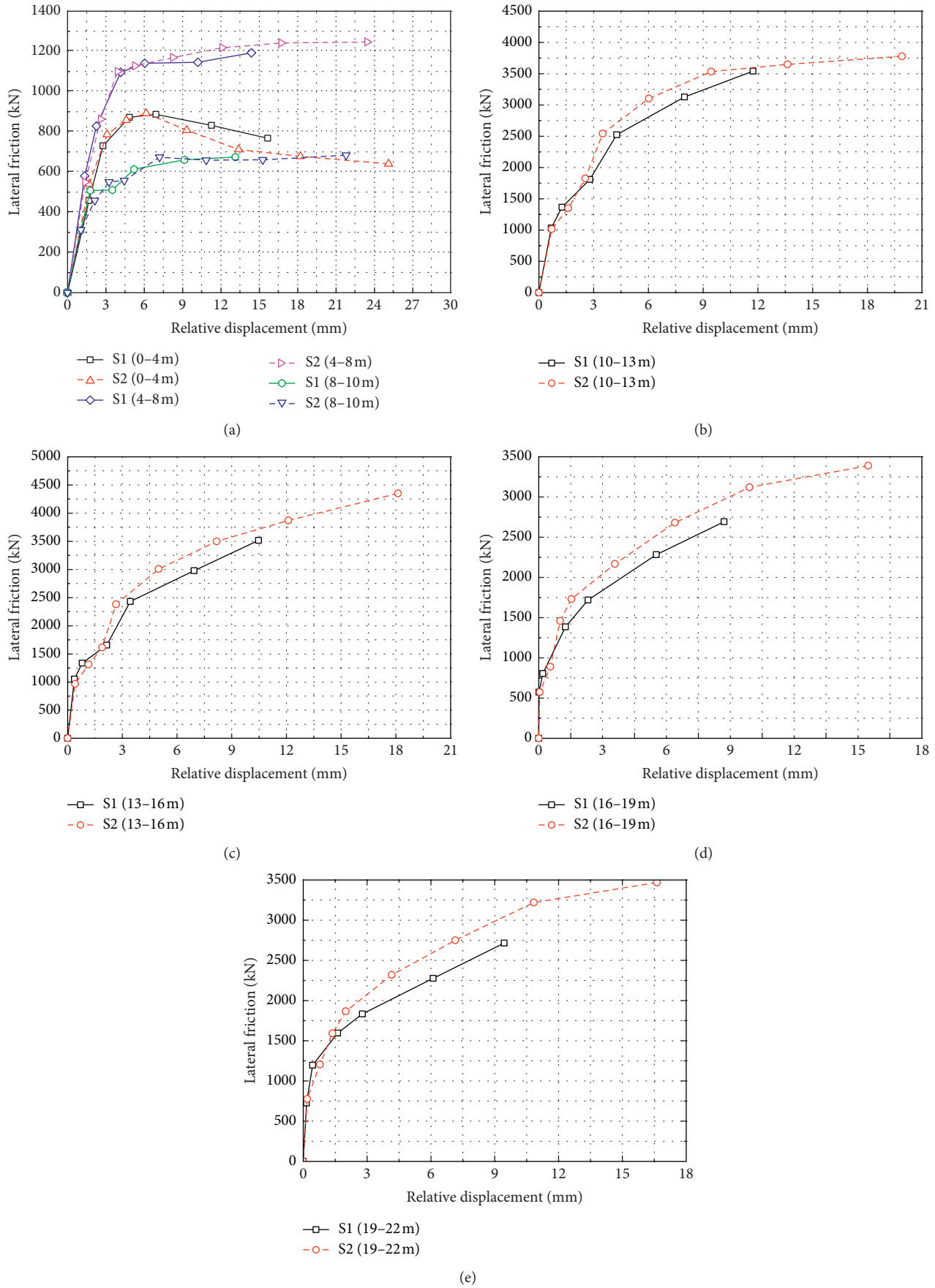

Figure 5: Relative displacement curve: part of (a) 1–10 m, (b) 10–13 m, (c) 13–16 m, (d) 16–19 m, and (e) 19–22 m.

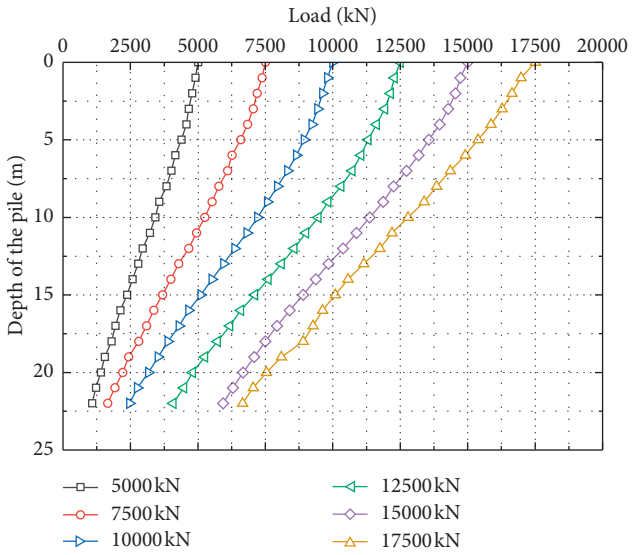

Figure 6: Axial force curve of S1.

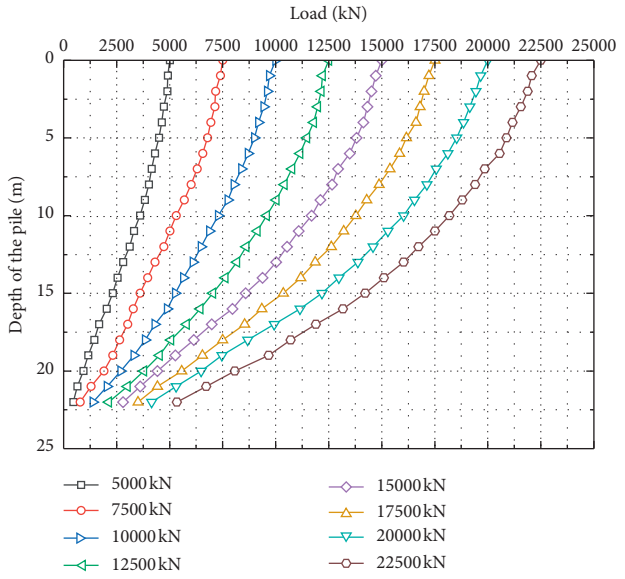

Figure 7: Axial force curve of S2.

and the relative displacement of the pile and soil decreases, which results in the overall settlement of the test pile being slowed down and the lateral friction is brought into play to a greater extent. And according to Figure 8, the lateral friction resistance of S2 along the pile length increases by 30.10%, 40.22%, 42.07%, 55.23%, 61.97%, 66.27%, and 69.36%, respectively, compared with S1 under their respective ultimate loads.

3.4. Height of Slurry Climbing. The soil around the pile will be squeezed in the process of slurry climbing. The compression of the soil around the pile (i.e., the pore between the pile and the soil) can be calculated by the theory of column hole expansion, and the equilibrium equation will be as follows [35]:

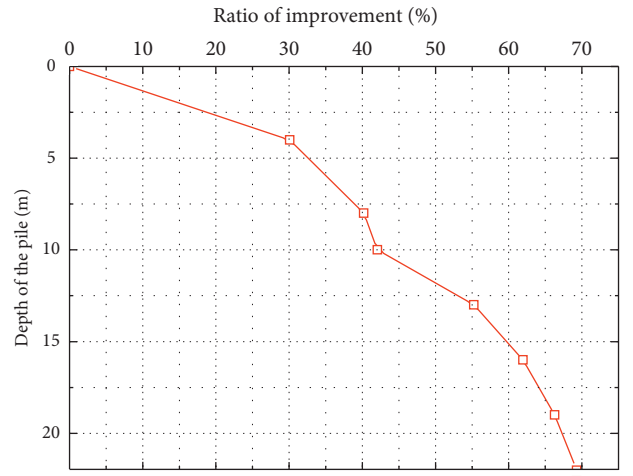

Figure 8: Curve of pile lateral friction increases proportion along pile depth.

$$r\frac{d\sigma_r}{dr} + (\sigma_r - \sigma_\theta) = 0. \tag{1}$$

The boundary conditions:

$$\sigma_r(a) = p, \quad \lim_{r\longrightarrow\infty} \sigma_r = p_0. \tag{2}$$

The geometric equations:

$$\begin{aligned} \varepsilon_r &= -\frac{du_r}{dr}, \\ \varepsilon_\theta &= -\frac{u_r}{r}. \end{aligned} \tag{3}$$

The constitutive equations:

$$\varepsilon_r = \frac{1-v^2}{E}\left(\sigma_r - \frac{v}{1-v}\sigma_\theta\right), \tag{4}$$

$$\varepsilon_\theta = \frac{1-v^2}{E}\left(\sigma_\theta - \frac{v}{1-v}\sigma_r\right). \tag{5}$$

The displacement of soil on the side of pile is obtained:

$$\delta = \frac{p-p_0}{2G}\left(\frac{a}{r}\right)^2 r, \tag{6}$$

where σ_r is the radial stress, σ_θ is the tangential stress, r is the radius of pile, D is the diameter of pile, p is the grouting pressure, p_0 is the initial stress of soil, G is the shear modulus and $G = E/(2(1+v))$, E is the modulus of elasticity, and v is Poisson's ratio.

Because the drilling hole is formed by rotary drilling, the influence of mud skin on the side of pile is neglected, taking $r = a = D/2$, and the displacement of soil on the side of pile is as follows:

$$\delta = \frac{(p-p_0)D}{4G}. \tag{7}$$

The flow of cement slurry on the pile side can be regarded as a non-Newtonian fluid. The relationship between pressure difference and shear stress during the flow of

cement slurry and the equation of uniformity is as follows [36]:

$$\tau = \frac{\Delta p r}{2L}, \tag{8}$$

$$\tau_w = \frac{\Delta p}{2L} R, \tag{9}$$

$$\tau_0 = \frac{\Delta p_0 R}{2L}. \tag{10}$$

where τ is the shear stress, τ_w is the shear stress at the edge of cracks, τ_0 is the shear stress yield value, L is the pile length, δ is the displacement of soil on the side of pile, r is the radius of pile and $R = (r + \delta)$, Δp is the pressure difference, and Δp_0 is the pressure difference when shear stress equals the yield value.

The condition for Bingham fluid to flow in the pipeline is $\Delta p > \Delta p_0$.

For the non-time-dependent viscous fluid, the constitutive equations are as follows:

$$\dot{\gamma} = f(\tau), \quad \text{or} \left(-\frac{du}{dr} = f(\tau) \right). \tag{11}$$

The Bingham fluid equation is used in the process of cement slurry flow, and its rheological equation can be written as follows:

$$f(\tau) = \frac{1}{\eta_p} (\tau - \tau_0). \tag{12}$$

If we define the boundary conditions ($r = R$, $u = 0$), then equation (11) can be written as follows:

$$u = \int_r^R f(\tau) d r. \tag{13}$$

Given equation (9), equation (8) can be rewritten as follows:

$$\tau = \frac{\tau_w}{R} r. \tag{14}$$

Given equation (14), equation (13) can be rewritten as follows:

$$u = \frac{R}{\tau_w} \int_\tau^{\tau_w} f(\tau) d\tau. \tag{15}$$

Given equation (12), equation (15) can be rewritten as follows:

$$u = \frac{R}{2\eta_p \tau_w} \left[\tau_w^2 - \tau^2 - 2\tau_0 (\tau_w - \tau) \right]. \tag{16}$$

By substituting equation (8) and equation (9) into (16), velocity of flow can be rewritten as follows:

$$u = \frac{\Delta p}{4L\eta_p} \left(R^2 - r^2 \right) - \frac{\tau_0}{\eta_p} (R - r), \tag{17}$$

where u is the velocity of flow and η_p is the plastic viscosity.

Flow rate:

$$Q = \int_0^R 2\pi r u \, dr = 2\pi \int_0^R r u \, dr. \tag{18}$$

If we define the boundary conditions ($r = R$, $u = 0$), then equation (18) can be rewritten as follows:

$$Q = \int_0^R \pi r^2 f(\tau) dr. \tag{19}$$

By substituting equation (12), equation (14), and equation (17) into (19), the flow rate can be rewritten as follows:

$$Q = \frac{\pi \Delta p R^4}{8L\eta_p} \left(1 - \frac{4r}{3R} \right). \tag{20}$$

The mean velocity of Bingham fluid under the laminar flow is considered as follows:

$$v = \frac{R^2}{8L\eta_p} \left(\Delta p - \frac{8\tau_0 L}{3R} \right). \tag{21}$$

So the pressure difference is as follows:

$$\Delta p = \frac{32\eta_p L v}{D^2} + \frac{16\tau_0 L}{3D}. \tag{22}$$

To ensure that the slurry continues climbing after reaching a certain height on the side of the pile, the slurry pressure should be greater than the splitting pressure between the pile and the soil. When the slurry pressure is less than the splitting pressure, the slurry will stop climbing, and the height at this time is the maximum climbing height of the slurry. According to formula (22) and the condition of slurry climbing, the height of climbing is 10.7 m after the soil is segmented and iterated. This is very approximate to the 12 m obtained from the field test, which shows that the theoretical analysis model has good applicability.

4. Discussion

4.1. Mechanism of Interaction between Cement Grout and Soil. Cement grout often acts on soil in various forms. Its action form is related to the types of grout, grouting technology, rheological properties, grout parameters, and soil properties. Forms can also be transformed or coexisted with each other, such as splitting or infiltration in the process of compaction. The main forms are compaction, splitting, and infiltration.

4.1.1. Compaction. Grout is forced to squeeze into the soil at the end of the pile through the grouting pipe, thus forming a spherical or block distribution at the end of the pile, also known as the grout bulb. When the grout continues to be injected, the volume of the grout bulb increases continuously, resulting in the larger uplift force, which squeezes the surrounding soil and improves the soil conditions near the pile end.

4.1.2. Splitting. The grout injected at the end of pile compacts the surrounding soil under the pressure. The soil

begins to split after the pressure is enough to overcome the resistance of the soil. The grout flows along the splitting surface and forms linear, reticulate, and vein-shaped cementation in the soil, which has the effect of reinforcing the soil and increases the strength of the foundation.

4.1.3. Infiltration. Under the action of grouting pressure, the grout extrudes free water and gas to infiltrate into the soil pore at the pile end and the interface between pile and soil. The larger the grouting pressure is, the larger the diffusion distance of grout is. When the grout solidifies, the soil particles are cemented into a whole, enhancing the strength of the soil at the end of the pile remarkably.

4.2. Mechanism of Postgrouting to Increase Bearing Capacity. The positive effect of the postgrouting technology at the pile end can be summarized as follows:

(1) Under the pressure of grouting, the cement grout compacts the soil at the end of the pile, forms a reinforcement zone, and enhances the bearing capacity.

(2) The cement grout solidifies the sediment and eliminates the mud around the pile, thus significantly improving the performance of soil and improving the lateral friction.

(3) Because of the seepage and splitting effect of grouting, the mechanical properties of the soil at the pile end have been significantly improved.

The grouting effect is shown in Figure 9.

4.2.1. Increasing the Strength of Bearing Strata. The infiltration, compaction, and splitting effects of the grout significantly enhance the strength and mechanical properties of the bearing strata. In the loess area, when the grouting pressure is greater than the splitting pressure of the soil, the homogeneous soil and grout form a high-strength composite, greatly improving the stability of the whole pile foundation.

4.2.2. Increasing the End Resistance. The grout penetrates into the pile end under the pressure and then begins to form the pile end reinforcement zone together with the surrounding soil. The formation of reinforcing zone enlarges the stress area and greatly increases the resistance at the pile end. Owing to the increasing grouting pressure, the reinforcing zone produces upward force on the pile end, which makes the grout rising continuously and the pile rising slowly. At this time, the downward friction resistance will be formed, which is equivalent to apply the prestressing at the pile end. Therefore, under the axial load, the end resistance will be brought into play ahead of time.

4.2.3. Enhancing the Lateral Friction. During the construction of bored piles, the lateral friction is easily affected by many unfavorable factors such as the mud around the pile, water, and concrete necking [37]. Postgrouting at the pile end can effectively weaken and eliminate these adverse effects and significantly improve the characteristics of the pile-soil interface. In the process of grouting, with the increased grouting pressure and grouting volume, part of the grout overflows and penetrates into the gap between the pile and surrounding soil [38, 39]. After solidification, the strength of soil is increased significantly, which greatly improves the lateral friction.

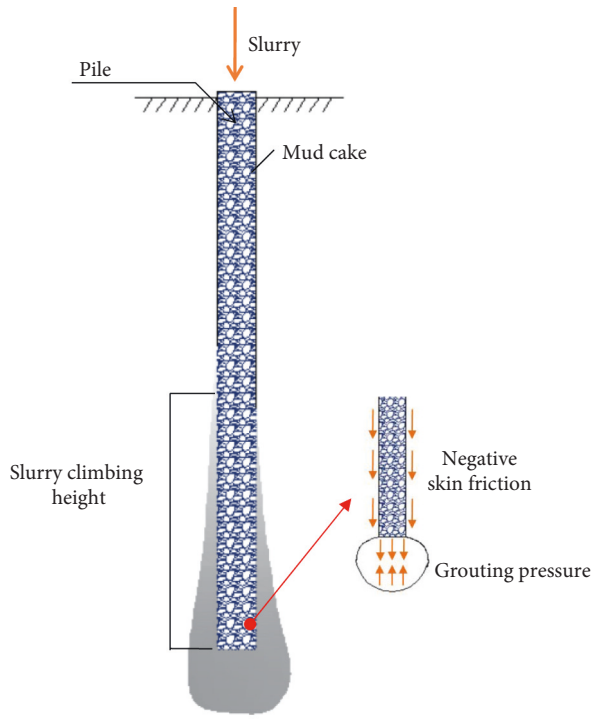

Figure 9: Schematic diagram of the postgrouting effect.

5. Conclusions

(1) The postgrouting increases the strength of the soil at the pile end and decreases the pile settlement under the load. The bearing capacity of pile foundation is 28.57% higher than that of the conventional pile. Under the same load condition, the settlement of the postgrouting pile is less than that of the conventional pile, and when the load of the pile top is 17500 kN, the settlement of pile foundation is 26.19% less than that of the conventional pile.

(2) The relative displacement of pile and soil in the climbing part of grout decreases, promoting the exertion of the lateral friction to a greater extent. Meanwhile, the lateral friction of each part of the pile is increased, and the increase effect decreases upward along the pile end. Under the ultimate load, the value of lateral friction is increased by 16.31% compared with the conventional pile.

(3) Postgrouting causes the phenomenon of grouting climbing. Theoretical calculation shows that the climbing height of the slurry is 10.7 m, which is close to the experimental results.

(4) The main forms of action of soil and grout are compaction, splitting, and infiltration. The mechanism of postgrouting at the pile end to improve the bearing capacity of pile foundation is mainly embodied in the improvement of end resistance and lateral friction by increasing the strength of bearing strata and boosting the performance of the pile-soil interface.

Data Availability

Data supporting this research article are available from the corresponding author on request.

Conflicts of Interest

The authors declare that they have no conflicts of interest.

Acknowledgments

The authors gratefully acknowledge the financial support by the National Key R&D problem of China (no. 2018YFC0808706) and the Project on Social Development of Shaanxi Provincial Science (no. 2018SF-378).

References

[1] Y. Shang, F. Niu, X. Wu, and M. Liu, "A novel refrigerant system to reduce refreezing time of cast-in-place pile foundation in permafrost regions," *Applied Thermal Engineering*, vol. 128, pp. 1151–1158, 2018.

[2] S. C. Reddy and A. W. Stuedlein, "Serviceability limit state reliability-based design of augered cast-in-place piles in granular soils," *Canadian Geotechnical Journal*, vol. 54, no. 12, pp. 1704–1715, 2017.

[3] J. Lai, H. Liu, J. Qiu, and J. Chen, "Settlement analysis of saturated tailings dam treated by CFG pile composite foundation," *Advances in Materials Science and Engineering*, vol. 2016, Article ID 7383762, 10 pages, 2016.

[4] Z. F. Wang, J. S. Shen, and W. C. Cheng, "Simple method to predict ground displacements caused by installing horizontal jet-grouting columns," *Mathematical Problems in Engineering*, vol. 2018, Article ID 1897394, 11 pages, 2018.

[5] Y. Li, S. Xu, H. Liu, E. Ma, and L. Wang, "Displacement and stress characteristics of tunnel foundation in collapsible loess ground reinforced by jet grouting columns," *Advances in Civil Engineering*, vol. 2018, Article ID 2352174, 16 pages, 2018.

[6] J. Lai, H. Liu, J. Qiu et al., "Stress analysis of CFG pile composite foundation in consolidating saturated mine tailings dam," *Advances in Materials Science and Engineering*, vol. 2016, Article ID 3948754, 12 pages, 2016.

[7] Y. You, J. Wang, Q. Wu et al., "Causes of pile foundation failure in permafrost regions: the case study of a dry bridge of the Qinghai-Tibet Railway," *Engineering Geology*, vol. 230, pp. 95–103, 2017.

[8] Q.-Q. Zhang and Z.-M. Zhang, "A simplified nonlinear approach for single pile settlement analysis," *Canadian Geotechnical Journal*, vol. 49, no. 11, pp. 1256–1266, 2012.

[9] Q.-Q. Zhang and Z.-M. Zhang, "Simplified calculation approach for settlement of single pile and pile groups," *Journal of Computing in Civil Engineering*, vol. 26, no. 6, pp. 750–758, 2012.

[10] Q. Q. Zhang, Z. M. Zhang, and J. Y. He, "A simplified approach for settlement analysis of single pile and pile groups considering interaction between identical piles in multilayered soils," *Computers and Geotechnics*, vol. 37, no. 7-8, pp. 969–976, 2010.

[11] L. Wang, B. He, Y. Hong, Z. Guo, and L. Li, "Field tests of the lateral monotonic and cyclic performance of jet-grouting-reinforced cast-in-place piles," *Journal of Geotechnical and Geoenvironmental Engineering*, vol. 141, no. 5, 2015.

[12] J. Zhou, X. Zhang, H. S. Jiang, C. Lyu, and E. Oh, "Static and dynamic load tests of shaft and base grouted concrete piles," *Advances in Civil Engineering*, vol. 2017, Article ID 2548020, 11 pages, 2017.

[13] A.-H. Karimi and A. Eslami, "Physical modelling for pile performance combined with ground improvement using frustum confining vessel," *International Journal of Physical Modelling in Geotechnics*, vol. 18, no. 3, pp. 162–174, 2018.

[14] A. H. Karimi, A. Eslami, M. Zarrabi, and J. Khazaei, "Study of pile behavior by improvement of confining soils using frustum confining vessel," *Scientia Iranica*, vol. 24, no. 4, pp. 1874–1882, 2017.

[15] J. Khazaei and A. Eslami, "Postgrouted helical piles behavior through physical modeling by FCV," *Marine Georesources & Geotechnology*, vol. 35, no. 4, pp. 528–537, 2016.

[16] S. Thiyyakkandi, M. McVay, D. Bloomquist, and P. Lai, "Measured and predicted response of a new jetted and grouted precast pile with membranes in cohesionless Soils," *Journal of Geotechnical and Geoenvironmental Engineering*, vol. 139, no. 8, pp. 1334–1345, 2013.

[17] X. Liu, K. Fang, Z. Zhang, and Q. Zhang, "Prestressing effect evaluation for a grouted shaft: a case study," *Proceedings of the Institution of Civil Engineers—Geotechnical Engineering*, vol. 167, no. 3, pp. 253–261, 2015.

[18] G. Dai, W. Gong, X. Zhao, and X. Zhou, "Static testing of pile-base post-grouting piles of the Suramadu Bridge," *Geotechnical Testing Journal*, vol. 34, no. 1, pp. 34–49, 2011.

[19] S. Thiyyakkandi, M. Mcvay, and P. Lai, "Experimental group behavior of grouted deep foundations," *Geotechnical Testing Journal*, vol. 37, no. 4, 2014.

[20] H. Youn and F. Tonon, "Numerical analysis on post-grouted drilled shafts: a case study at the Brazo River Bridge, TX," *Computers and Geotechnics*, vol. 37, no. 4, pp. 456–465, 2010.

[21] B. He, L. Z. Wang, and H. Yi, "Capacity and failure mechanism of laterally loaded jet-grouting reinforced piles: field and numerical investigation," *Science China Technological Sciences*, vol. 59, no. 5, pp. 763–776, 2016.

[22] M. Zarrabi and A. Eslami, "Behavior of piles under different installation effects by physical modeling," *International Journal of Geomechanics*, vol. 16, no. 5, 2016.

[23] K. Fang, Z. Zhang, and Q. Yang, "Response evaluation of axially loaded grouted drilled shaft," *Marine Georesources & Geotechnology*, vol. 32, no. 2, pp. 123–134, 2014.

[24] Q.-Q. Zhang, Z.-M. Zhang, and S.-C. Li, "Investigation into skin friction of bored pile including influence of soil strength at pile base," *Marine Georesources & Geotechnology*, vol. 31, no. 1, pp. 1–16, 2013.

[25] Y. Zheng, J. Xiong, T. Liu, X. Yue, and J. Qiu, "Performance of a deep excavation in lanzhou strong permeable sandy gravel strata," *Arabian Journal of Geosciences*, vol. 12, no. 16, p. 12, 2019.

[26] J. Qiu, Y. Qin, Z. Feng, L. Wang, and K. Wang, "Safety risks and protection measures for the city wall during the construction and operation of Xi'an metro," *Journal of Performance of Constructed Facilities*, vol. 33, no. 5, p. 12, 2019.

[27] J. Qiu, X. Wang, J. Lai, Q. Zhang, and J. Wang, "Response characteristics and preventions for seismic subsidence of loess

in Northwest China," *Natural Hazards*, vol. 92, no. 3, pp. 1909–1935, 2018.

[28] H. Sun, Q. P. Wang, P. Zhang, Y. J. Zhong, and X. B. Yue, "Spatiotemporal characteristics of tunnel traffic accidents in China from 2001 to present," *Advances in Civil Engineering*, vol. 2019, Article ID 4536414, 16 pages, 2019.

[29] S. B. Zhang, S. Y. He, J. L. Qiu, W. Xu, R. Garnes, and L. X. Wang, "Displacement characteristics of a urban tunnel in silty soil by shallow tunnelling method," *Advances in Civil Engineering*, vol. 2019, Article ID. 3975745, 15 pages, 2019.

[30] L. Duan, Y. Zhang, and J. Lai, "Influence of ground temperature on shotcrete-to-rock adhesion in tunnels," *Advances in Materials Science and Engineering*, vol. 2019, Article ID. 8709087, 18 pages,, 2019.

[31] Q. Q. Zhang, S. C. Li, and Z. M. Zhang, "Influence of reaction piles on test pile response in a static load test," *Journal of Zhejiang University-Science A*, vol. 14, no. 3, pp. 198–205, 2013.

[32] X. Yue, Y. Xie, H. Zhang, Y. Niu, S. Zhang, and J. Li, "Study on geotechnical characteristics of marine soil at Hong Kong-Zhuhai-Macao tunnel," *Marine Georesources & Geotechnology*, vol. 37, no. 8, pp. 1–12, 2019.

[33] Q.-Q. Zhang, S.-C. Li, and L.-P. Li, "Field and theoretical analysis on the response of destructive pile subjected to tension load," *Marine Georesources & Geotechnology*, vol. 33, no. 1, pp. 12–22, 2015.

[34] Z. Zhou, Y. Dong, P. Jiang, D. Han, and T. Liu, "Calculation of pile side friction by multiparameter statistical analysis," *Advances in Civil Engineering*, vol. 2019, Article ID 2638520, 12 pages, 2019.

[35] H.-S. Yu, *Cavity Expansion Methods in Geomechanics*, Science Press, Beijing, China, 2013.

[36] Z. Wang, Y. Xie, H. Liu, and Z. Feng, "Analysis on deformation and structural safety of a novel concrete-filled steel tube support system in loess tunnel," *European Journal of Environmental and Civil Engineering*, vol. 22, pp. 1–21, 2018.

[37] Q. Zhang and Z. Zhang, "Study on interaction between dissimilar piles in layered soils," *International Journal for Numerical and Analytical Methods in Geomechanics*, vol. 35, no. 1, pp. 67–81, 2011.

[38] X. L. Luo, X. Meng, W. J. Gan, and Y. H. Chen, "Traffic data imputation algorithm based on improved low rank matrix decomposition," *Journal of Sensors*, vol. 2019, Article ID 7092713, 10 pages, 2019.

[39] X. X. Nie, S. S. Feng, S. D. Zhang, and Q. Gan, "Simulation study on the dynamic ventilation control of single head roadway in high- altitude mine based on thermal comfort," *Advances in Civil Engineering*, vol. 2019, Article ID 2973504, 12 pages, 2019.